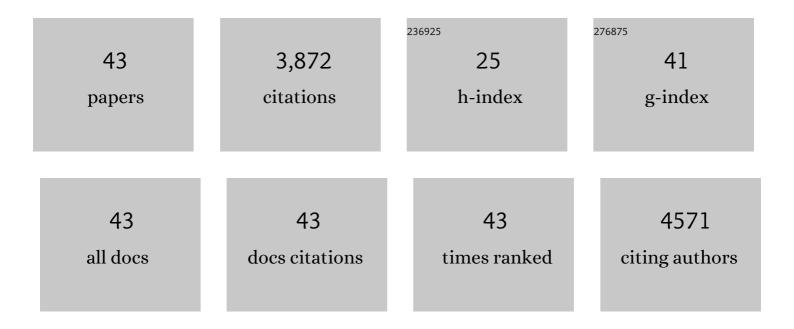
Hideo Ago

List of Publications by Year in descending order

Source: https://exaly.com/author-pdf/6721601/publications.pdf Version: 2024-02-01



HIDEO ACC

#	Article	IF	CITATIONS
1	Native structure of photosystem II at 1.95ÂÃ resolution viewed by femtosecond X-ray pulses. Nature, 2015, 517, 99-103.	27.8	1,050
2	Crystal structure of the RNA-dependent RNA polymerase of hepatitis C virus. Structure, 1999, 7, 1417-1426.	3.3	381
3	An oxyl/oxo mechanism for oxygen-oxygen coupling in PSII revealed by an x-ray free-electron laser. Science, 2019, 366, 334-338.	12.6	248
4	Cloning and Crystal Structure of Hematopoietic Prostaglandin D Synthase. Cell, 1997, 90, 1085-1095.	28.9	244
5	Determination of damage-free crystal structure of an X-ray–sensitive protein using an XFEL. Nature Methods, 2014, 11, 734-736.	19.0	237
6	Structural Basis of the Substrate-specific Two-step Catalysis of Long Chain Fatty Acyl-CoA Synthetase Dimer. Journal of Biological Chemistry, 2004, 279, 31717-31726.	3.4	189
7	Determination of Damage-free Crystal Structure of an X-ray Sensitive Protein Using XFEL. Nihon Kessho Gakkaishi, 2015, 57, 122-128.	0.0	158
8	Crystal structure of a human membrane protein involved in cysteinyl leukotriene biosynthesis. Nature, 2007, 448, 609-612.	27.8	140
9	Crystal Structure of Squid Rhodopsin with Intracellularly Extended Cytoplasmic Region. Journal of Biological Chemistry, 2008, 283, 17753-17756.	3.4	122
10	Novel Features of Eukaryotic Photosystem II Revealed by Its Crystal Structure Analysis from a Red Alga. Journal of Biological Chemistry, 2016, 291, 5676-5687.	3.4	100
11	Structural Basis of the Sphingomyelin Phosphodiesterase Activity in Neutral Sphingomyelinase from Bacillus cereus. Journal of Biological Chemistry, 2006, 281, 16157-16167.	3.4	82
12	Capturing an initial intermediate during the P450nor enzymatic reaction using time-resolved XFEL crystallography and caged-substrate. Nature Communications, 2017, 8, 1585.	12.8	74
13	A nanosecond time-resolved XFEL analysis of structural changes associated with CO release from cytochrome c oxidase. Science Advances, 2017, 3, e1603042.	10.3	68
14	Crystal structure of annexin V with its ligand K-201 as a calcium channel activity inhibitor. Journal of Molecular Biology, 1997, 274, 16-20.	4.2	60
15	The essential role of C-terminal residues in regulating the activity of hepatitis C virus RNA-dependent RNA polymerase. Biochimica Et Biophysica Acta - Proteins and Proteomics, 2002, 1601, 38-48.	2.3	59
16	Structural Basis of Leukotriene B4 12-Hydroxydehydrogenase/15-Oxo-prostaglandin 13-Reductase Catalytic Mechanism and a Possible Src Homology 3 Domain Binding Loop. Journal of Biological Chemistry, 2004, 279, 22615-22623.	3.4	58
17	Protein microcrystallography using synchrotron radiation. IUCrJ, 2017, 4, 529-539.	2.2	56
18	An isomorphous replacement method for efficient de novo phasing for serial femtosecond crystallography. Scientific Reports, 2015, 5, 14017.	3.3	54

Hideo Ago

#	Article	IF	CITATIONS
19	Helix 8 of the Leukotriene B4 Receptor Is Required for the Conformational Change to the Low Affinity State after G-protein Activation. Journal of Biological Chemistry, 2003, 278, 41500-41509.	3.4	52
20	The First Crystal Structure of Archaeal Aldolase. Journal of Biological Chemistry, 2003, 278, 10799-10806.	3.4	42
21	Crystal Structure of a Novel FAD-, FMN-, and ATP-containing l-Proline Dehydrogenase Complex from Pyrococcus horikoshii. Journal of Biological Chemistry, 2005, 280, 31045-31049.	3.4	39
22	Development of a dose-limiting data collection strategy for serial synchrotron rotation crystallography. Journal of Synchrotron Radiation, 2017, 24, 29-41.	2.4	39
23	Structural Basis of the Catalytic Mechanism Operating in Open-Closed Conformers of Lipocalin Type Prostaglandin D Synthase. Journal of Biological Chemistry, 2009, 284, 22344-22352.	3.4	38
24	The Catalytic Architecture of Leukotriene C4 Synthase with Two Arginine Residues. Journal of Biological Chemistry, 2011, 286, 16392-16401.	3.4	29
25	An unprecedented dioxygen species revealed by serial femtosecond rotation crystallography in copper nitrite reductase. IUCrJ, 2018, 5, 22-31.	2.2	27
26	Oxyanion Hole-stabilized Stereospecific Isomerization in Ribose-5-phosphate Isomerase (Rpi). Journal of Biological Chemistry, 2003, 278, 49183-49190.	3.4	26
27	An unprecedented insight into the catalytic mechanism of copper nitrite reductase from atomic-resolution and damage-free structures. Science Advances, 2021, 7, .	10.3	25
28	Catalytically important damage-free structures of a copper nitrite reductase obtained by femtosecond X-ray laser and room-temperature neutron crystallography. IUCrJ, 2019, 6, 761-772.	2.2	24
29	Experimental phase determination with selenomethionine or mercury-derivatization in serial femtosecond crystallography. IUCrJ, 2017, 4, 639-647.	2.2	24
30	Crystal Structure of Anti-Configuration of Indomethacin and Leukotriene B4 12-Hydroxydehydrogenase/15-Oxo-Prostaglandin 13-Reductase Complex Reveals the Structural Basis of Broad Spectrum Indomethacin Efficacy. Journal of Biochemistry, 2006, 140, 457-466.	1.7	21
31	Cloning, Expression, Crystallization, and Preliminary X-Ray Analysis of Recombinant Mouse Lipocalin-type Prostaglandin D Synthase, a Somnogen-Producing Enzyme. Journal of Biochemistry, 2003, 133, 29-32.	1.7	20
32	XFEL Crystal Structures of Peroxidase Compound II. Angewandte Chemie - International Edition, 2021, 60, 14578-14585.	13.8	18
33	Internally bridging water molecule in transmembrane α-helical kink. Current Opinion in Structural Biology, 2010, 20, 456-463.	5.7	17
34	A leukotriene C4 synthase inhibitor with the backbone of 5-(5-methylene-4-oxo-4,5-dihydrothiazol-2-ylamino) isophthalic acid. Journal of Biochemistry, 2013, 153, 421-429.	1.7	13
35	Application of maximum-entropy maps in the accurate refinement of a putative acylphosphatase using 1.3â€Ã X-ray diffraction data. Acta Crystallographica Section D: Biological Crystallography, 2008, 64, 237-247.	2.5	9
36	A temperature-controlled cold-gas humidifier and its application to protein crystals with the humid-air and glue-coating method. Journal of Applied Crystallography, 2019, 52, 699-705.	4.5	9

Hideo Ago

#	Article	IF	CITATIONS
37	Seleno-detergent MAD phasing of leukotriene C ₄ synthase in complex with dodecyl-β- <scp>D</scp> -selenomaltoside. Acta Crystallographica Section F: Structural Biology Communications, 2011, 67, 1666-1673.	0.7	7
38	A new sesquiterpene from Nicotiana umbratica Burbidge. Tetrahedron, 1997, 53, 11563-11568.	1.9	4
39	A nearly on-axis spectroscopic system for simultaneouslyÂmeasuring UV–visible absorption and X-ray diffraction in the SPring-8 structural genomics beamline. Journal of Synchrotron Radiation, 2016, 23, 334-338.	2.4	4
40	Crystallization and preliminary diffraction studies of prostaglandin E ₂ -specific monoclonal antibody Fab fragment in the ligand complex. Acta Crystallographica Section F: Structural Biology Communications, 2008, 64, 1027-1030.	0.7	3
41	Radiation Damage-Free Structure of Photosystem II Determined by Femtosecond X-Ray Free Electron Laser Pulses. Nihon Kessho Gakkaishi, 2016, 58, 126-132.	0.0	1
42	Recent Advances in Biology of Crysteinyl Leukotriene. Nihon Kessho Gakkaishi, 2010, 52, 69-75.	0.0	1
43	XFEL Crystal Structures of Peroxidase Compound II. Angewandte Chemie. 2021, 133, 14699-14706.	2.0	0